



Published in final edited form as:

Circulation. 2016 May 3; 133(18): 1783–1794. doi:10.1161/CIRCULATIONAHA.115.020617.

In Pulmonary Arterial Hypertension, Reduced BMPR2 Promotes Endothelial-to-Mesenchymal Transition via HMGA1 and its Target Slug

Rachel K. Hopper, MD^{1,2}, Jan-Renier A.J. Moonen, MD, PhD^{1,3}, Isabel Diebold, MD¹, Aiqin Cao, PhD¹, Christopher J. Rhodes, PhD¹, Nancy F. Tojais, PhD¹, Jan K. Hennigs, MD¹, Mingxia Gu, MD, PhD¹, Lingli Wang, MD¹, and Marlene Rabinovitch, MD¹

¹Department of Pediatrics, the Vera Moulton Wall Center for Pulmonary Vascular Disease and the Cardiovascular Institute, Stanford University School of Medicine, Stanford, CA ²Department of Pediatrics, Perelman School of Medicine at the University of Pennsylvania and Children's Hospital of Philadelphia, Philadelphia, PA ³Center for Congenital Heart Diseases, Department of Pediatric Cardiology, University Medical Center Groningen, University of Groningen, the Netherlands

Abstract

Background—We previously reported high-throughput RNA sequencing analyses that identified heightened expression of the chromatin architectural factor High Mobility Group AT-hook 1 (HMGA1) in pulmonary arterial (PA) endothelial cells (ECs) from idiopathic PA hypertension (IPAH) patients compared to controls. Since HMGA1 promotes epithelial to mesenchymal transition in cancer, we hypothesized that increased HMGA1 could induce transition of PAECs to a smooth muscle (SM)-like mesenchymal phenotype (EndMT), explaining both dysregulation of PAEC function and possible cellular contribution to the occlusive remodeling that characterizes advanced IPAH.

Methods and Results—We documented increased HMGA1 in PAECs cultured from IPAH vs. donor control lungs. Confocal microscopy of lung explants localized the increase in HMGA1 consistently to PA endothelium, and identified many cells double-positive for HMGA1 and smooth muscle 22 alpha (SM22 α) in occlusive and plexogenic lesions. Since decreased expression and function of bone morphogenetic protein receptor (BMPR)2 is observed in PAH, we reduced BMPR2 by siRNA in control PAECs and documented an increase in HMGA1 protein. Consistent with transition of PAECs by HMGA1, we detected reduced PECAM-1 (CD31) and increased EndMT markers, α SMA, SM22 α , calponin, phospho-vimentin and Slug. The transition was associated with spindle SM-like morphology, and the increase in α SMA was largely reversed by joint knockdown of BMPR2 and HMGA1 or Slug. Pulmonary ECs from mice with EC-specific loss of BMPR2 showed similar gene and protein changes.

Correspondence: Marlene Rabinovitch, MD, Stanford University School of Medicine, CCSR-1215A, 269 Campus Drive, Stanford, CA 94305, Phone: 650-723-6928, Fax: 650-723-6700, marlener@stanford.edu.

Disclosures: None.

Conclusions—Increased HMGA1 in PAECs resulting from dysfunctional BMPR2 signaling can transition endothelium to SM-like cells associated with PAH.

Keywords

HMGA1; Endothelial-to-Mesenchymal Transition; Pulmonary Hypertension

Introduction

Pulmonary arterial hypertension (PAH), whether idiopathic (IPAH), heritable (HPAH) or associated with other conditions (APAH) is a potentially lethal disease characterized by progressive vascular changes leading to obliteration of distal pulmonary arteries (PAs)¹. Abnormal muscularization and loss of pre-capillary PAs is followed by proliferation of vascular cells in more proximal PAs to form an occlusive neointima². The origin of the neointimal cells remains unclear; they were originally thought to be derived from the muscular media as they express alpha smooth muscle actin (α SMA)³. However dysfunctional endothelial cells (ECs) could, by endothelial-to-mesenchymal transition (EndMT)^{4,5} contribute to neointima formation either directly, or indirectly by transforming in a way that impedes their ability to produce factors such as apelin that control smooth muscle cell (SMC) proliferation⁶.

EndMT is a process by which endothelial cells acquire a mesenchymal phenotype in association with expression of SMC genes, such as α SMA⁴ and phospho(p) vimentin, and reduction in endothelial genes such as VE-cadherin and PECAM-1 (CD144 and CD31, respectively). Endothelial fate-mapping in a mouse model of pulmonary hypertension demonstrated cells of endothelial lineage expressing SMC markers that contribute to the neointima⁷. Pulmonary artery endothelial cells (PAECs) can acquire a smooth muscle phenotype in culture in a transforming growth factor beta (TGF β)-dependent manner^{8,9}. While EndMT has been implicated in the human pathology of PAH⁵, the initiating factor and the pathway involved have not been described.

Our group applied high throughput RNA sequencing to PAECs obtained from lungs of patients with PAH or from donor controls, and observed elevated mRNA expression of High Mobility Group AT-hook 1 (HMGA1) in the patients¹⁰. This gene is a member of a family of architectural factors that bind AT-rich regions of DNA and alter the chromatin structure to influence transcriptional activity¹¹. HMGA1 is highly expressed in stem cells during embryonic development, but as tissues mature HMGA1 levels drop and are very low in fully differentiated tissues¹¹. Abnormal elevation in HMGA1 contributes to neoplastic transformation in multiple cancers¹²⁻¹⁴ by inducing epithelial-to-mesenchymal transition (EMT)¹². An invasive phenotype results from repression of the epithelial junction protein E-cadherin and up-regulation of mesenchymal genes. These features completely reverse with loss of HMGA1¹⁴. Snail and Slug (Snai1 and Snai2, respectively) are closely related zinc finger transcription factors that have been implicated in EMT and EndMT¹⁵⁻¹⁷. HMGA2, a protein closely related to HMGA1, can directly affect expression of Snail by binding the promoter and recruiting SMAD proteins to increase transcription of the *SNAIL* gene¹⁸.

BMPR2 mutations are found in approximately 70% of patients with heritable PAH and 20% of sporadic cases or IPAH^{19,20}, and even IPAH patients without known BMPR2 mutations have reduced expression of BMPR2, as do patients with APAH²¹. Silencing BMPR2 in control PAECs causes an elevation in expression of HMGA1 that is phenocopied by reducing levels of β -catenin, an effector of gene regulation downstream of BMPR2¹⁰. We therefore hypothesized that dysfunctional BMPR2 signaling in PAH PAECs causes an elevation in HMGA1, promoting acquisition of a mesenchymal phenotype via a process of EndMT.

Materials and Methods

Subjects and human primary cell culture

As previously described²², we harvested and cultured ECs predominantly from small (<1mm) PAs. We analyzed tissue sections from explanted lungs of patients with IPAH and HPAH, obtained at time of transplantation, and from unused donor control lungs, via the Pulmonary Hypertension Breakthrough Initiative (PHBI) Network, funded by the Cardiovascular Medical and Education Fund (CMREF) and NIH-NHLBI. Demographic and clinical data relevant to PAH patients and controls are in Table 1. PAECs from lung tissues were grown in commercial EC media containing 5% FBS (ScienCell, Carlsbad, CA) and used at passages 3–6²² as were commercial human PAECs (PromoCell, Heidelberg, Germany).

siRNA transfection

siRNAs for BMPR2, HMGA1, Slug and non-targeting control siRNAs (GE Healthcare Dharmacon, Lafayette, CO) were transfected into subconfluent PAECs at a concentration of 20nM using Lipofectamine RNAiMAX and OptiMEM medium (Life Technologies, Carlsbad, CA). We measured gene expression (mRNA) at 72h and protein levels at seven days. In some experiments, PAECs were transfected with control non-targeting siRNA, incubated for 48h, and then treated with TGF β 2 (Abcam, Cambridge, MA) for five days.

Quantitative RT-PCR

RNA was extracted using a spin column-based kit (Zymo Research, Irvine, CA) and quantified using a spectrophotometer. Quantitative RT-PCR (qPCR) was performed on a CFX384 Real Time System (BioRad, Hercules, CA) using 4ng cDNA, 1mM primers, and a SybrGreen master mix (Life Technologies). Primer sequences, designed using NCBI's Primer-BLAST function, are shown in Supplementary Table 1.

Immunoblotting

Protein samples were separated by SDS-PAGE on 4–12% Bis-Tris gradient gels (Life Technologies), transferred onto nitrocellulose membranes (Bio-Rad), and incubated with primary antibodies, diluted 1:1,000 (unless noted): rabbit anti-HMGA1 (1:10,000), rabbit anti-vimentin (1:4,000), mouse anti-phospho vimentin (1:250), mouse anti-PECAM-1, rabbit anti-Snail/Slug, rabbit VE-cadherin, goat anti-SM22 α (Abcam), mouse anti- α SMA (Sigma-Aldrich, St Louis, MO), mouse anti-GAPDH, mouse anti- β -actin (Santa Cruz

Biotechnology, Dallas, TX), and mouse anti-BMP2 (1:200, BD Biosciences, Franklin Lakes, NJ).

Immunohistochemistry

Formaldehyde-fixed, paraffin-embedded tissue sections were stained as previously described²², using an HMGA1 antibody (1:500, Abcam) and anti-rabbit secondary antibody 3,3'-diaminobenzidine (Dako, Carpinteria, CA), and counterstained with hematoxylin.

Immunofluorescence

Tissue sections were processed as described above and incubated with antibodies against HMGA1 (1:500, Abcam), von Willebrand Factor (1:100, Abcam) and SM22 α (1:100, Abcam). Nuclei were stained with DRAQ7 (Biostatus, UK). PAECs were cultured in chamber slides, fixed in 4% paraformaldehyde and permeabilized using 0.1% Triton X-100 (Sigma-Aldrich). Slides were incubated with primary antibodies against α SMA (1:200, Sigma-Aldrich) and VE-cadherin (1:150, Abcam). Fluorescent-tagged secondary antibodies were used at 1:400 (Life Technologies). Slides were mounted using Vectashield with or without DAPI (Vector Laboratories, Burlingame, CA) and imaged using a confocal microscope (Olympus, Center Valley, PA and Leica, Buffalo Grove, IL).

Transgenic Mice

The Animal Care Committee of Stanford University approved all protocols. Mice with an endothelial-specific inducible knockout of BMP2 were created in our laboratory (SCL-*CreER*^{TM4}/*R26R/Bmpr2*^{-/-})²³. Wild-type mice were used as controls. Murine pulmonary ECs were isolated from digested whole lung tissue using CD31 antibody-coated magnetic beads (Dynabeads; Invitrogen) as previously described⁶.

Statistical Analysis

Values from multiple experiments are depicted in box plots showing minimum, maximum and the median for each experiment. When values are depicted in scatterplots, the lines represent the mean \pm SEM. The number of experiments, IPAH or control cells used are indicated in the figure legends. Statistical significance was determined using one-way ANOVA followed by Bonferroni's multiple comparisons test or by Kruskal-Wallis test followed by Dunn's post hoc test, as indicated in the figure legends. When only two groups were compared, statistical differences were assessed with unpaired two-tailed Student's *t*-test. A *p*-value of <0.05 was considered significant.

Results

HMGA1 is elevated in PAECs from patients with PAH relative to controls

We observed elevated HMGA1 protein in PAECs (passage 3–6) from HPAH patients with a BMP2 mutation compared to those from donor control lungs and a similar trend in PAECs from IPAH patients (Fig 1A). HMGA1 immunoperoxidase staining was prominent in the PA endothelium of lung tissue sections from IPAH patients whereas immunoreactivity was barely detectable in control PA endothelium (Fig 1B). While HMGA1 was localized to the

endothelium primarily, HMGA1 positive cells also appeared in the neointima, often close to the endothelial surface of the occluded vessels (Fig 1C). HMGA1 immunoreactivity was increased in PAs of all sizes in PAH vs. control lungs and in all lesions including plexiform lesions, (Fig 1C, D).

To determine whether HMGA1 was co-expressed with endothelial and/or SM markers in IPAH PAs, we performed confocal microscopy on lung tissue sections using immunofluorescence staining. In vessels of different sizes from PAH patients, HMGA1 appeared to co-localize predominantly with the endothelial marker von Willebrand Factor (vWF) but also with smooth muscle 22 alpha (SM22 α) positive cells in the neointima (Fig 2). HMGA1 expression was much less intense in control tissues.

Loss of BMPR2 induces elevation of HMGA1 and changes consistent with EndMT

To mimic BMPR2 loss in PAH patients, we transfected BMPR2 siRNA in control PAECs and evaluated whether, as a result of elevated HMGA1 previously shown¹⁰, EndMT transcription factors Snail and Slug, and smooth muscle markers would be increased and endothelial markers reduced. BMPR2 siRNA resulted in an increase in HMGA1, Slug, α SMA and calponin mRNA, but there was no significant change in VE-cadherin or Snail (Fig 3A). We confirmed loss of BMPR2 protein by immunoblot, and the associated elevation in HMGA1, increased Snail/Slug, α SMA and a prominent marker of EndMT, p-vimentin (Fig 3B,C). PECAM-1 was reduced (Fig 3C) but not VE-cadherin (Fig 3B). There was no change in another marker of EndMT, Twist (data not shown), suggesting that Snail/Slug are the critical transcription factors regulating EndMT resulting from loss of BMPR2.

Increased α SMA in PAECs transfected with BMPR2 siRNA was visualized using immunofluorescent staining and confocal microscopy (Fig 4A). Although VE-cadherin was not reduced by loss of BMPR2, we observed fragmented VE-cadherin immunostaining on the borders of PAECs suggesting an early breakdown of the junctions (Fig 4A). Consistent with this was the change in morphology of a subset of siBMPR2 treated PAECs, from the typical cobblestone appearance to an elongated, spindle shape (Fig 4B). Many of these elongated cells stained positively for α SMA (Fig 4C).

EndMT changes induced by loss of BMPR2 require HMGA1 and Slug

To determine whether HMGA1 was required for the EndMT induced by loss of BMPR2 we silenced BMPR2 and HMGA1, individually and in combination (Fig 5A). As loss of BMPR2 increases HMGA1 mRNA, we also found that loss of HMGA1 increased BMPR2 mRNA, suggesting a feedback mechanism (Fig 5A). The increase in Slug mRNA seen with loss of BMPR2 was abolished by co-transfection with siRNA for HMGA1 and BMPR2, indicating that Slug is a target of elevated HMGA1 resulting from loss of BMPR2. Similarly, the increase in α SMA mRNA caused by loss of BMPR2 was significantly abrogated by knockdown of both BMPR2 and HMGA1. Protein levels were similar to mRNA levels (Fig 5B). To determine whether Slug was required for the increase in α SMA expression, we silenced BMPR2 and Slug, individually and in combination (Fig 5C). We found that the increase in α SMA induced by loss of BMPR2 was completely prevented by concomitant knockdown of Slug mRNA, indicating that Slug is required for EndMT. Similar to our

observation with HMGA1, silencing Slug alone significantly increased BMPR2 mRNA suggesting that Slug plays a role in the feedback mechanism regulated by HMGA1 (Fig 5C).

EndMT changes are not replicated by TGF α treatment

To determine whether loss of BMPR2 induces an increase in TGF β signaling that is necessary for EndMT, we treated control PAECs with TGF β 2, previously implicated in EndMT²⁴. TGF β 2 signaling increased phosphorylated SMAD2 relative to total SMAD2 but loss of BMPR2 did not phosphorylate SMAD2 (Fig 6). Moreover TGF β 2 increased HMGA1 but did not induce the EndMT related increase in Snail/Slug or α SMA (Fig 6). Taken together, our results show that EndMT changes in PAECs associated with loss of BMPR2 are not acting via TGF β 2 signaling.

Mice lacking endothelial BMPR2 show changes consistent with EndMT

To further characterize the relationship between reduced BMPR2 expression and EndMT, we studied EC-specific BMPR2 knockout mice (EC-BMPR2-KO) produced by breeding SCL-CreERTM, R26LacZ^{fl/fl} and *Bmpr2*^{fl/fl} mice and characterized in a previous study²³. They have no significant pulmonary hypertension at baseline, but develop exaggerated right ventricular systolic pressure and right ventricular hypertrophy following exposure to chronic hypoxia²³ and do not reverse pulmonary hypertension after recovery in room air²⁵. Pulmonary ECs isolated from these mice show increased expression of HMGA1 and Slug at the mRNA and protein level, relative to wild type (WT) mice (Fig 7A, B). While the increase in α SMA mRNA was small and not accompanied by a significant elevation in protein level, the increase in SM22 α was particularly prominent both at mRNA and protein level (Fig 7A, B). Immunofluorescence microscopy, however, showed a distinct increase in expression of α SMA in EC-BMPR2-KO relative to WT pulmonary ECs (Fig 7C). Taken together, these findings suggest that loss of BMPR2 in pulmonary ECs is sufficient to promote features of EndMT in a transgenic mouse that develops more severe disease in response to a pulmonary hypertension-producing stimulus.

Discussion

Our study identifies a novel role for HMGA1 in promoting EndMT in PAH. We show that PAECs highly expressing HMGA1 are prevalent in human PAH PA lesions. Moreover, HMGA1 is upregulated by loss of BMPR2 in PAECs, as assessed either using siRNA to reduce BMPR2 in cultured human PAECs, or in transgenic mice with BMPR2 deleted in ECs. Downstream effectors of the increase in HMGA1 suggest an axis in which induction of Slug increases expression of α SMA and other SM genes including SM22 α and calponin (see schema in Figure 8).

Previous studies have documented elevated expression of HMGA1 in response to insults in human umbilical endothelial cells, with HMGA1 regulating genes induced by hypoxia²⁶ and viral infection/inflammation²⁷. An elevation in HMGA1 is also a feature of angiogenesis in post-ischemia brain ECs²⁸. Following identification of elevated HMGA1 mRNA in isolated PAECs of patients with PAH by RNAseq¹⁰, we sought to determine the role of elevated HMGA1 particularly with regard to EndMT in IPAH.

HMGA1 co-localized primarily with endothelial and occasionally with smooth muscle markers in arteries with neointimal formation and plexogenic lesions. While a previous study in mice used fate mapping to show α SMA-positive cells of endothelial lineage within the neointima, these cells comprised only a small sub-population⁷. Similarly, not all neointimal cells in the human tissue expressed p-vimentin, a marker of EndMT. Thus, it is possible that, at best, only a subset of PAECs contribute to the SM-like cells of the neointima as has been previously reported^{5,7}. The majority of PAECs may be transformed in a manner that impairs their ability to produce inhibitors of SMC proliferation, such as apelin^{6,29}. Consistent with this, we showed that PAH ECs produce less apelin when compared to donor controls⁵. This transition without transformation is in keeping with mesenchymal changes noted in epithelial cells injured in fibrotic lung disease³⁰. These cells promote fibrosis but do not become fibroblasts. It is conceivable that once ECs fully undergo EndMT, HMGA1 levels fall and are not detectable by immunofluorescence. This is in keeping with the drop in HMGA1 levels seen normally in tissue differentiation in development^{31,32}, but different from HMGA1 expression in cancer cells undergoing EMT, which remains highly expressed¹⁴.

Clinical and experimental studies have linked reduced expression of BMPR2 to the development of PAH^{33,34}. Loss of BMPR2 in ECs confers susceptibility to apoptosis as well as impaired EC function as evidenced by angiogenesis and migration assays^{35,36}. We demonstrate a novel relationship between loss of BMPR2 and increased expression of HMGA1 that is associated with morphologic changes and increased expression of Slug, α SMA and other SMC proteins. These morphologic changes in cultured cells are in keeping with transmission electron microscopy studies of endothelial cells in the PAs from patients with PAH, that show increased microfilament bundles, consistent with cytoskeletal changes of EndMT³⁷. The high expression of HMGA1 in vWF-positive endothelial cells might suggest that HMGA1 can, as in cancer cells, contribute to the development of an apoptosis-resistant phenotype^{13,38}.

We previously related increased HMGA1 to elevated β -catenin¹⁰ resulting from loss of BMPR2. Other transcription factors or microRNAs (miRs) may be also involved. We investigated several miRs that are reduced in PAH, including miR 21^{39,40} and miR 26a⁴¹, but they do not appear to regulate HMGA1 (data not shown).

Co-transfection of siRNAs targeting HMGA1 and BMPR2 completely prevented the increase in Slug but only partially prevented the increase in α SMA at the mRNA and protein level. The incomplete repression of α SMA by HMGA1 siRNA vs. Slug siRNA in the context of loss of BMPR2 was surprising. Perhaps another factor elicited by HMGA1 knockdown tempers the loss of Slug-related genes. HMGA1 was not previously identified as a regulator of α SMA, but it could potentiate serum response factor (SRF)-dependent transcription as has been shown for HMGA1 and SM22 α ⁴².

Activation of BMPR2 signaling by BMP ligands reversed EMT in renal fibrosis⁴³ and EndMT in cardiac fibrosis⁴⁴. In mesenchymal breast cancer cells, silencing HMGA1 promoted mesenchymal-to-epithelial transition in conjunction with decreased proliferation, migration and invasion of the tumor cells¹⁴. Stimulation of PAECs with BMP9 does repress

HMGA1 (data not shown) suggesting that amplification of BMPR2 signaling via treatment with BMP9⁴⁵, FK506²³ or elafin⁴⁶ may reverse EndMT.

TGF β signaling induces EndMT in experimental models of kidney⁴⁷ and cardiac⁴⁴ fibrosis and mature bovine PAECs in culture have been shown to undergo EndMT in response to TGF β ⁸. However, loss of BMPR2 did not result in activation of SMAD2, and TGF β was insufficient to induce EndMT, highlighting a potentially unique feature of human PAECs.

Gene expression changes consistent with EndMT were verified in mice with an inducible loss of endothelial BMPR2 and isolated pulmonary ECs from these mice showed a propensity to undergo EndMT in culture (Fig 7). These mice showed mildly exaggerated pulmonary hypertension in chronic hypoxia²³, and could not reverse pulmonary hypertension upon return to normoxia, in association with fewer distal vessels that were highly muscularized²⁵. Thus the susceptibility to EndMT may impair recovery from a pulmonary hypertensive state.

In addition to EndMT, HMGA1 overexpression in cancer cells targets inflammatory genes, increases reactive oxygen species, and reduces mitochondrial DNA repair efficiency^{48,49}, features that we observed in PAECs from patients with BMPR2 mutation²⁵. HMGA1 is thought to act as a transcriptional regulator, linking inflammatory pathways with oncogenic potential. In PAH, HMGA1 may be the pivotal link between the “pro-inflammatory” state of PAECs and the breakdown of endothelial junctions due to EndMT, that permits inflammatory cell infiltration of the vessel wall^{22,50} and propagation of the neointima. Thus HMGA1 induces EndMT causing endothelial dysfunction and possible cellular contribution to occlusive vascular changes.

Supplementary Material

Refer to Web version on PubMed Central for supplementary material.

Acknowledgments

The co-authors would especially like to acknowledge the outstanding scientific contribution of the second author, Dr. Jan-Renier A. J. Moonen who, over the past year, carried out major revisions requiring additional experiments, repeat statistical analyses, and redrafting of many of the Figures. IPAH and control lung tissues provided by the PHBI were procured at the Transplant Procurement Centers at Allegheny Hospital, Baylor University, The Cleveland Clinic, Stanford University, University of California-San Diego, Vanderbilt University and the University of Alabama at Birmingham, and de-identified patient data were obtained via the Data Coordinating Center at the University of Michigan. The authors are very grateful to Dr. Michal Bental Roof for assistance with preparation of the manuscript and to Dr. Lu Tian for statistical consultation.

Funding Sources: RKH was supported by Pediatric Heart Center Research Program, Lucile Packard Children’s Hospital, Lucile Packard Foundation for Children’s Health, Stanford CTSA (grant UL1 RR025744); JRM by the Netherlands Heart Foundation (Grant 2013T116) and Netherlands CardioVascular Research Initiative (CVON): the Dutch Heart Foundation, Dutch Federation of University Medical Centers, the Netherlands Organization for Health Research and Development, and the Royal Netherlands Academy of Sciences (CVON Phaedra 2012-08). ID was funded by the Deutsche Herzstiftung e.V (S/06/11) and JKH, by a fellowship of the Deutsche Forschungsgemeinschaft (He 6855/1-1). MR is funded by NIH/NHLBI grants 5U01 HL107393 and R24 HL123767, the Cardiovascular Medical Research and Education Fund (CMREF) Grant UL1RR024986, and the Dunlevie Chair in Pediatric Cardiology at Stanford University.

References

1. Pietra GG, Edwards WD, Kay JM, Rich S, Kernis J, Schloo B, Ayres SM, Bergofsky EH, Brundage BH, Detre KM. Histopathology of primary pulmonary hypertension. A qualitative and quantitative study of pulmonary blood vessels from 58 patients in the National Heart, Lung, and Blood Institute, Primary Pulmonary Hypertension Registry. *Circulation*. 1989; 80:1198–1206. [PubMed: 2805258]
2. Rabinovitch M. Molecular pathogenesis of pulmonary arterial hypertension. *J Clin Invest*. 2012; 122:4306–4313. [PubMed: 23202738]
3. Jones PL, Cowan KN, Rabinovitch M. Tenascin-C, proliferation and subendothelial fibronectin in progressive pulmonary vascular disease. *Am J Pathol*. 1997; 150:1349–1360. [PubMed: 9094991]
4. Arciniegas E, Frid MG, Douglas IS, Stenmark KR. Perspectives on endothelial-to-mesenchymal transition: potential contribution to vascular remodeling in chronic pulmonary hypertension. *Am J Physiol Lung Cell Mol Physiol*. 2007; 293:L1–L8. [PubMed: 17384082]
5. Ranchoux B, Antigny F, Rucker-Martin C, Hautefort A, Péchoux C, Bogaard HJ, Dorfmueller P, Remy S, Lecerf F, Planté S, Chat S, Fadel E, Houssaini A, Anegon I, Adnot S, Simonneau G, Humbert M, Cohen-Kaminsky S, Perros F. Endothelial-to-Mesenchymal Transition in Pulmonary Hypertension. *Circulation*. 2015; 131:1006–1018. [PubMed: 25593290]
6. Alastalo T-P, Li M, Perez V, de J, Pham D, Sawada H, Wang JK, Koskenvuo M, Wang L, Freeman BA, Chang HY, Rabinovitch M. Disruption of PPAR γ / β -catenin-mediated regulation of apelin impairs BMP-induced mouse and human pulmonary arterial EC survival. *J Clin Invest*. 2011; 121:3735–3746. [PubMed: 21821917]
7. Qiao L, Nishimura T, Shi L, Sessions D, Thrasher A, Trudell JR, Berry GJ, Pearl RG, Kao PN. Endothelial Fate Mapping in Mice With Pulmonary Hypertension. *Circulation*. 2014; 129:692–703. [PubMed: 24201301]
8. Arciniegas E, Sutton AB, Allen TD, Schor AM. Transforming growth factor beta 1 promotes the differentiation of endothelial cells into smooth muscle-like cells in vitro. *J Cell Sci*. 1992; 103:521–529. [PubMed: 1478952]
9. Frid MG, Kale VA, Stenmark KR. Mature Vascular Endothelium Can Give Rise to Smooth Muscle Cells via Endothelial-Mesenchymal Transdifferentiation In Vitro Analysis. *Circ Res*. 2002; 90:1189–1196. [PubMed: 12065322]
10. Rhodes CJ, Im H, Cao A, Hennigs JK, Wang L, Sa S, Chen P-I, Nickel NP, Miyagawa K, Hopper RK, Tojais NF, Li CG, Gu M, Spiekerkoetter E, Xian Z, Chen R, Zhao M, Kaschwich M, del Rosario PA, Bernstein D, Zamanian RT, Wu JC, Snyder MP, Rabinovitch M. RNA Sequencing Analysis Detection of a Novel Pathway of Endothelial Dysfunction in Pulmonary Arterial Hypertension. *Am J Respir Crit Care Med*. 2015; 192:356–366. [PubMed: 26030479]
11. Sgarra R, Zammiti S, Lo Sardo A, Maurizio E, Arnoldo L, Pegoraro S, Giancotti V, Manfioletti G. HMGA molecular network: From transcriptional regulation to chromatin remodeling. *Biochim Biophys Acta BBA Gene Regul Mech*. 2010; 1799:37–47.
12. Silvia, Pegoraro S, Ros G, Piazza S, Sommaggio R, Ciani Y, Rosato A, Sgarra R, Del Sal G, Manfioletti G. HMGA1 promotes metastatic processes in basal-like breast cancer regulating EMT and stemness. *Oncotarget*. 4:1293–1308.
13. Wood LJ, Maher JF, Bunton TE, Resar LM. The oncogenic properties of the HMG-I gene family. *Cancer Res*. 2000; 60:4256–4261. [PubMed: 10945639]
14. Shah SN, Cope L, Poh W, Belton A, Roy S, Talbot CC, Sukumar S, Huso DL, Resar LMS. HMGA1: a master regulator of tumor progression in triple-negative breast cancer cells. *PloS One*. 2013; 8:e63419. [PubMed: 23658826]
15. Savagner P, Yamada KM, Thiery JP. The Zinc-Finger Protein Slug Causes Desmosome Dissociation, an Initial and Necessary Step for Growth Factor–induced Epithelial–Mesenchymal Transition. *J Cell Biol*. 1997; 137:1403–1419. [PubMed: 9182671]
16. Batlle E, Sancho E, Francé C, Domínguez D, Monfar M, Baulida J, García De Herreros A. The transcription factor snail is a repressor of E-cadherin gene expression in epithelial tumour cells. *Nat Cell Biol*. 2000; 2:84–89. [PubMed: 10655587]

17. Cano A, Pérez-Moreno MA, Rodrigo I, Locascio A, Blanco MJ, del Barrio MG, Portillo F, Nieto MA. The transcription factor snail controls epithelial-mesenchymal transitions by repressing E-cadherin expression. *Nat Cell Biol.* 2000; 2:76–83. [PubMed: 10655586]
18. Thuault S, Tan E-J, Peinado H, Cano A, Heldin C-H, Moustakas A. HMGA2 and Smads co-regulate SNAIL1 expression during induction of epithelial-to-mesenchymal transition. *J Biol Chem.* 2008; 283:33437–33446. [PubMed: 18832382]
19. Deng Z, Morse JH, Slager SL, Cuervo N, Moore KJ, Venetos G, Kalachikov S, Cayanis E, Fischer SG, Barst RJ, Hodge SE, Knowles JA. Familial Primary Pulmonary Hypertension (Gene PPH1) Is Caused by Mutations in the Bone Morphogenetic Protein Receptor–II Gene. *Am J Hum Genet.* 2000; 67:737–744. [PubMed: 10903931]
20. Lane KB, Machado RD, Pauciuolo MW, Thomson JR, Phillips JA, Loyd JE, Nichols WC, Trembath RC. International PPH Consortium. Heterozygous germline mutations in BMPR2, encoding a TGF-beta receptor, cause familial primary pulmonary hypertension. *Nat Genet.* 2000; 26:81–84. [PubMed: 10973254]
21. Atkinson C, Stewart S, Upton PD, Machado R, Thomson JR, Trembath RC, Morrell NW. Primary Pulmonary Hypertension Is Associated With Reduced Pulmonary Vascular Expression of Type II Bone Morphogenetic Protein Receptor. *Circulation.* 2002; 105:1672–1678. [PubMed: 11940546]
22. Sawada H, Saito T, Nickel NP, Alastalo T-P, Glotzbach JP, Chan R, Haghighat L, Fuchs G, Januszzyk M, Cao A, Lai Y-J, Perez V, de J, Kim Y-M, Wang L, Chen P-I, Spiekerkoetter E, Mitani Y, Gurtner GC, Sarnow P, Rabinovitch M. Reduced BMPR2 expression induces GM-CSF translation and macrophage recruitment in humans and mice to exacerbate pulmonary hypertension. *J Exp Med.* 2014; 211:263–280. [PubMed: 24446489]
23. Spiekerkoetter E, Tian X, Cai J, Hopper RK, Sudheendra D, Li CG, El-Bizri N, Sawada H, Haghighat R, Chan R, Haghighat L, de Jesus Perez V, Wang L, Reddy S, Zhao M, Bernstein D, Solow-Cordero DE, Beachy PA, Wandless TJ, Ten Dijke P, Rabinovitch M. FK506 activates BMPR2, rescues endothelial dysfunction, and reverses pulmonary hypertension. *J Clin Invest.* 2013; 123:3600–3613. [PubMed: 23867624]
24. Medici D, Potenta S, Kalluri R. Transforming growth factor- β 2 promotes Snail-mediated endothelial-mesenchymal transition through convergence of Smad-dependent and Smad-independent signalling. *Biochem J.* 2011; 437:515–520. [PubMed: 21585337]
25. Diebold I, Hennigs JK, Miyagawa K, Li CG, Nickel NP, Kaschwich M, Cao A, Wang L, Reddy S, Chen P-I, Nakahira K, Alcazar MAA, Hopper RK, Ji L, Feldman BJ, Rabinovitch M. BMPR2 Preserves Mitochondrial Function and DNA during Reoxygenation to Promote Endothelial Cell Survival and Reverse Pulmonary Hypertension. *Cell Metab.* 2015; 21:596–608. [PubMed: 25863249]
26. Ji Y-S, Xu Q, Schmedtje JF. Hypoxia Induces High-Mobility-Group Protein I(Y) and Transcription of the Cyclooxygenase-2 Gene in Human Vascular Endothelium. *Circ Res.* 1998; 83:295–304. [PubMed: 9710122]
27. Viemann D, Schmolke M, Lueken A, Boergeling Y, Friesenhagen J, Wittkowski H, Ludwig S, Roth J. H5N1 Virus Activates Signaling Pathways in Human Endothelial Cells Resulting in a Specific Imbalanced Inflammatory Response. *J Immunol.* 2011; 186:164–173. [PubMed: 21106851]
28. Camós S, Gubern C, Sobrado M, Rodríguez R, Romera VG, Moro MA, Lizasoain I, Serena J, Mallolas J, Castellanos M. The high-mobility group I-Y transcription factor is involved in cerebral ischemia and modulates the expression of angiogenic proteins. *Neuroscience.* 2014; 269:112–130. [PubMed: 24680881]
29. Chandra SM, Razavi H, Kim J, Agrawal R, Kundu RK, de Jesus Perez V, Zamanian RT, Quertermous T, Chun HJ. Disruption of the apelin-APJ system worsens hypoxia-induced pulmonary hypertension. *Arterioscler Thromb Vasc Biol.* 2011; 31:814–820. [PubMed: 21233449]
30. Yang J, Wheeler SE, Velikoff M, Kleaveland KR, LaFemina MJ, Frank JA, Chapman HA, Christensen PJ, Kim KK. Activated alveolar epithelial cells initiate fibrosis through secretion of mesenchymal proteins. *Am J Pathol.* 2013; 183:1559–1570. [PubMed: 24012677]
31. Brocher J, Vogel B, Hock R. HMGA1 down-regulation is crucial for chromatin composition and a gene expression profile permitting myogenic differentiation. *BMC Cell Biol.* 2010; 11:64. [PubMed: 20701767]

32. Chiappetta G, Avantiaggiato V, Visconti R, Fedele M, Battista S, Trapasso F, Merciai BM, Fidanza V, Giaccotti V, Santoro M, Simeone A, Fusco A. High level expression of the HMGI (Y) gene during embryonic development. *Oncogene*. 1996; 13:2439–2446. [PubMed: 8957086]
33. Song Y, Jones JE, Beppu H, Keane JF, Loscalzo J, Zhang Y-Y. Increased susceptibility to pulmonary hypertension in heterozygous BMP2-mutant mice. *Circulation*. 2005; 112:553–562. [PubMed: 16027259]
34. Hong K-H, Lee YJ, Lee E, Park SO, Han C, Beppu H, Li E, Raizada MK, Bloch KD, Oh SP. Genetic ablation of the BMP2 gene in pulmonary endothelium is sufficient to predispose to pulmonary arterial hypertension. *Circulation*. 2008; 118:722–730. [PubMed: 18663089]
35. Teichert-Kuliszewska K, Kutryk MJB, Kuliszewski MA, Karoubi G, Courtman DW, Zucco L, Granton J, Stewart DJ. Bone morphogenetic protein receptor-2 signaling promotes pulmonary arterial endothelial cell survival: implications for loss-of-function mutations in the pathogenesis of pulmonary hypertension. *Circ Res*. 2006; 98:209–217. [PubMed: 16357305]
36. De Jesus Perez VA, Alastalo T-P, Wu JC, Axelrod JD, Cooke JP, Amieva M, Rabinovitch M. Bone morphogenetic protein 2 induces pulmonary angiogenesis via Wnt-beta-catenin and Wnt-RhoA-Rac1 pathways. *J Cell Biol*. 2009; 184:83–99. [PubMed: 19139264]
37. Rabinovitch M, Bothwell T, Hayakawa BN, Williams WG, Trusler GA, Rowe RD, Olley PM, Cutz E. Pulmonary artery endothelial abnormalities in patients with congenital heart defects and pulmonary hypertension. A correlation of light with scanning electron microscopy and transmission electron microscopy. *Lab Invest J Tech Methods Pathol*. 1986; 55:632–653.
38. Masri FA, Xu W, Comhair SAA, Asosingh K, Koo M, Vasanthi A, Drazba J, Anand-Apte B, Erzurum SC. Hyperproliferative apoptosis-resistant endothelial cells in idiopathic pulmonary arterial hypertension. *Am J Physiol Lung Cell Mol Physiol*. 2007; 293:L548–L554. [PubMed: 17526595]
39. Yang S, Banerjee S, Freitas A, de Cui H, Xie N, Abraham E, Liu G. miR-21 regulates chronic hypoxia-induced pulmonary vascular remodeling. *Am J Physiol Lung Cell Mol Physiol*. 2012; 302:L521–529. [PubMed: 22227207]
40. Drake KM, Zygmunt D, Mavrikakis L, Harbor P, Wang L, Comhair SA, Erzurum SC, Aldred MA. Altered MicroRNA processing in heritable pulmonary arterial hypertension: an important role for Smad-8. *Am J Respir Crit Care Med*. 2011; 184:1400–1408. [PubMed: 21920918]
41. Schlosser K, White RJ, Stewart DJ. miR-26a linked to pulmonary hypertension by global assessment of circulating extracellular microRNAs. *Am J Respir Crit Care Med*. 2013; 188:1472–1475. [PubMed: 24328779]
42. Chin MT, Pellacani A, Wang H, Lin SSJ, Jain MK, Perrella MA, Lee M-E. Enhancement of Serum-response Factor-dependent Transcription and DNA Binding by the Architectural Transcription Factor HMG-I(Y). *J Biol Chem*. 1998; 273:9755–9760. [PubMed: 9545312]
43. Yang Y-L, Ju H-Z, Liu S-F, Lee T-C, Shih Y-W, Chuang L-Y, Guh J-Y, Yang Y-Y, Liao T-N, Hung T-J, Hung M-Y. BMP-2 suppresses renal interstitial fibrosis by regulating epithelial-mesenchymal transition. *J Cell Biochem*. 2011; 112:2558–2565. [PubMed: 21590708]
44. Zeisberg EM, Tarnavski O, Zeisberg M, Dorfman AL, McMullen JR, Gustafsson E, Chandraker A, Yuan X, Pu WT, Roberts AB, Neilson EG, Sayegh MH, Izumo S, Kalluri R. Endothelial-to-mesenchymal transition contributes to cardiac fibrosis. *Nat Med*. 2007; 13:952–961. [PubMed: 17660828]
45. Upton PD, Davies RJ, Trembath RC, Morrell NW. Bone Morphogenetic Protein (BMP) and Activin Type II Receptors Balance BMP9 Signals Mediated by Activin Receptor-like Kinase-1 in Human Pulmonary Artery Endothelial Cells. *J Biol Chem*. 2009; 284:15794–15804. [PubMed: 19366699]
46. Nickel NP, Spiekerkoetter E, Gu M, Li CG, Li H, Kaschwich M, Diebold I, Hennigs JK, Kim K-Y, Miyagawa K, Wang L, Cao A, Sa S, Jiang X, Stockstill RW, Nicolls MR, Zamarian RT, Bland RD, Rabinovitch M. Elafin Reverses Pulmonary Hypertension via Caveolin-1-Dependent Bone Morphogenetic Protein Signaling. *Am J Respir Crit Care Med*. 2015; 191:1273–1286. [PubMed: 25853696]
47. Li J, Qu X, Yao J, Caruana G, Ricardo SD, Yamamoto Y, Yamamoto H, Bertram JF. Blockade of endothelial-mesenchymal transition by a Smad3 inhibitor delays the early development of streptozotocin-induced diabetic nephropathy. *Diabetes*. 2010; 59:2612–2624. [PubMed: 20682692]

48. Schuldenfrei A, Belton A, Kowalski J, Talbot CC, Di Cello F, Poh W, Tsai H-L, Shah SN, Huso TH, Huso DL, Resar LMS. HMGA1 drives stem cell, inflammatory pathway, and cell cycle progression genes during lymphoid tumorigenesis. *BMC Genomics*. 2011; 12:549. [PubMed: 22053823]
49. Resar LMS. The high mobility group A1 gene: transforming inflammatory signals into cancer? *Cancer Res*. 2010; 70:436–439. [PubMed: 20068164]
50. Guignabert C, Alvira CM, Alastalo T-P, Sawada H, Hansmann G, Zhao M, Wang L, El-Bizri N, Rabinovitch M. Tie2-mediated loss of peroxisome proliferator-activated receptor-gamma in mice causes PDGF receptor-beta-dependent pulmonary arterial muscularization. *Am J Physiol Lung Cell Mol Physiol*. 2009; 297:L1082–1090. [PubMed: 19801450]

Author Manuscript

Author Manuscript

Author Manuscript

Author Manuscript

Clinical Perspectives

Linking the genetics of pulmonary arterial hypertension to endothelial mesenchymal transition of endothelial cells and to the formation of an occlusive neointima

Transition of endothelial cells to take on features of smooth muscle cells, a process called endothelial-to-mesenchymal transition (EndMT), is increasingly appreciated as a mechanism integral to vascular pathobiologies, including pulmonary arterial hypertension. The transformed endothelial cells may contribute to the expanding neointima either directly or by failing to produce inhibitors of smooth muscle cell proliferation. In this report we relate EndMT to reduced expression of the receptor for bone morphogenetic protein (BMP2) that occurs either related to a mutation or independent of a mutation in patients with pulmonary arterial hypertension (PAH). We show that loss of BMP2 causes an elevation in a chromatin remodeling and scaffolding protein, High Mobility Group AT-hook 1 (HMGA1) that has been implicated in transition of cancer cells. Elevated HMGA1 leads to an increase in a transcription factor called Slug that upregulates expression of smooth muscle genes such as smooth muscle actin and SM22 α . At the same time, impaired structure and reduced expression of endothelial cell junctional proteins, CD-31 (PECAM) and CD-144 (VE-Cadherin) respectively, lead to morphologic changes that promote the smooth muscle cell phenotype.

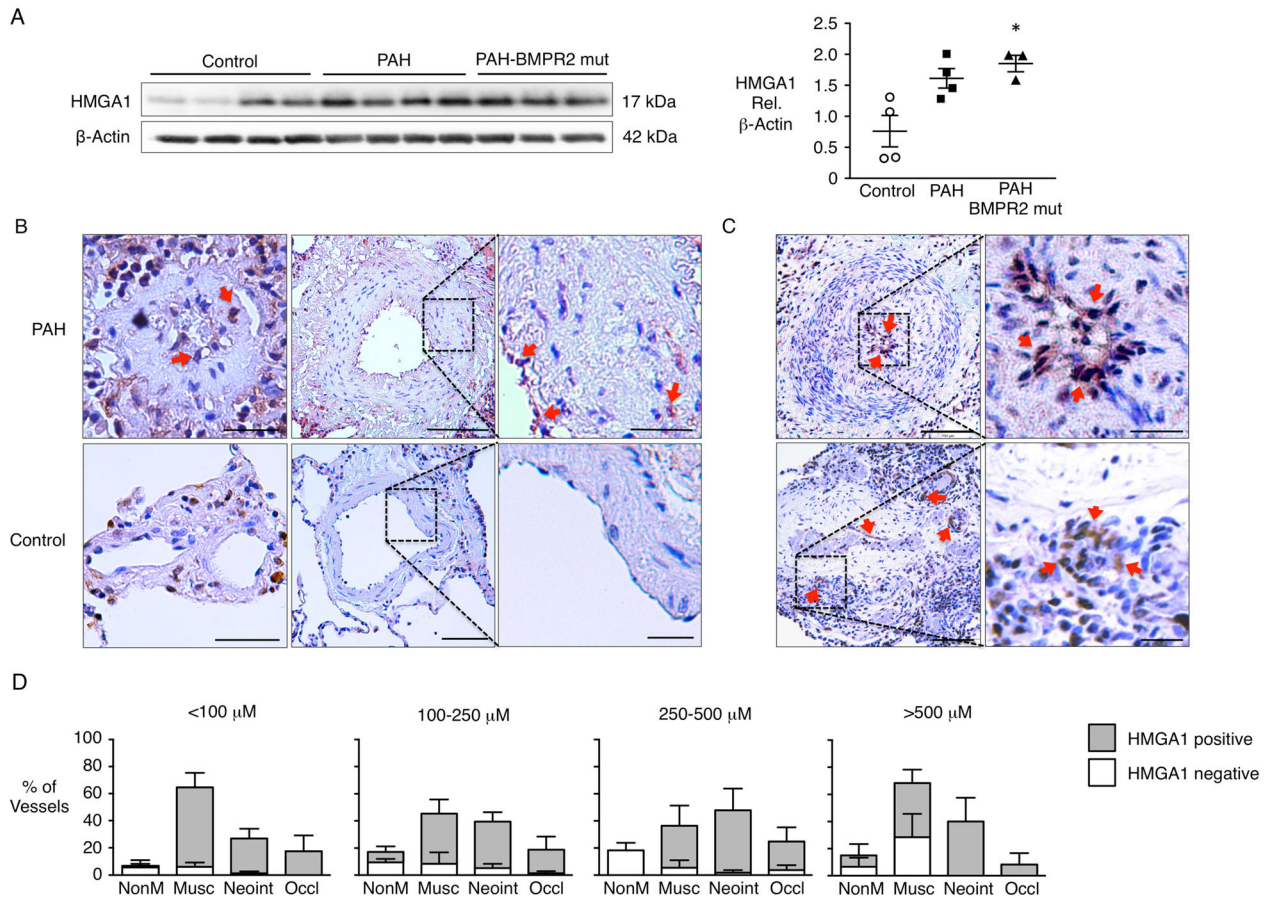


Figure 1.

Elevated HMGA1 protein expression in patients with PAH. (A) Western immunoblot and densitometric quantification of HMGA1 protein isolated from cultured PAECs from donor controls and patients with PAH with or without BMPR2 mutation. Scatterplots indicate mean \pm SEM. *P<0.05 compared to control by Kruskal-Wallis test with Dunn's post hoc testing. (B) Representative immunohistochemistry for HMGA1 (brown) and hematoxylin counterstain (blue-purple) in small peripheral (left panels) and larger pre-acinar pulmonary arteries (PAs) from controls and patients with PAH. In PAs from patients with PAH, HMGA1 was observed primarily in the endothelium and neointimal cells adjacent to the endothelium lining the vessel wall (arrows). The expression of HMGA1 was not detected by immunoperoxidase in the PA endothelium or the vascular wall from controls. Scale bar=50 μ m for the left images; 100 μ m for the center images and 25 μ m for the inserts. (C) Expression of HMGA1 is especially pronounced in the endothelium and neointimal cells of an occluded artery and in the endothelium of a plexiform lesion (arrows). Scale bar= 100 μ m and 25 μ m for the inserts. (D) Pulmonary tissues from patients with PAH were analyzed for histopathological signs of vascular disease in relation to HMGA1 expression. The degree of vascular disease was scored as absent (Normal); enhanced muscularization or medial hypertrophy (Musc); presence of neointimal hyperplasia (Neoint) or complete occlusion

(Occlud). Quantification of staining by vessel size is shown as mean±SEM for multiple vessels from n=3 patients with PAH.

Author Manuscript

Author Manuscript

Author Manuscript

Author Manuscript

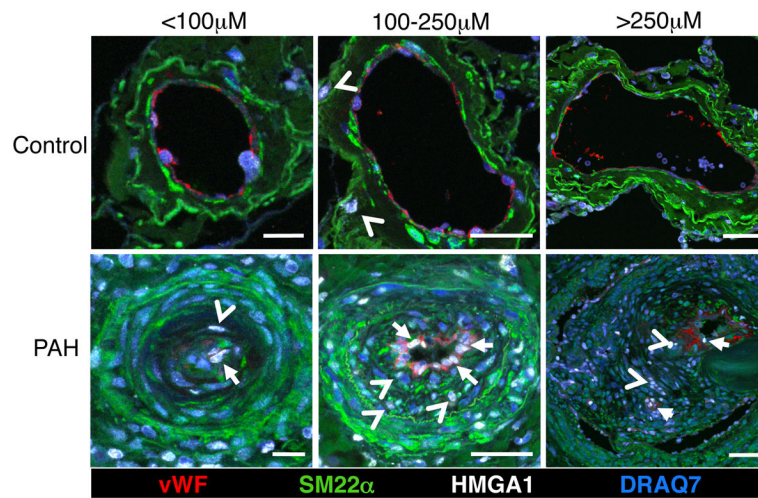
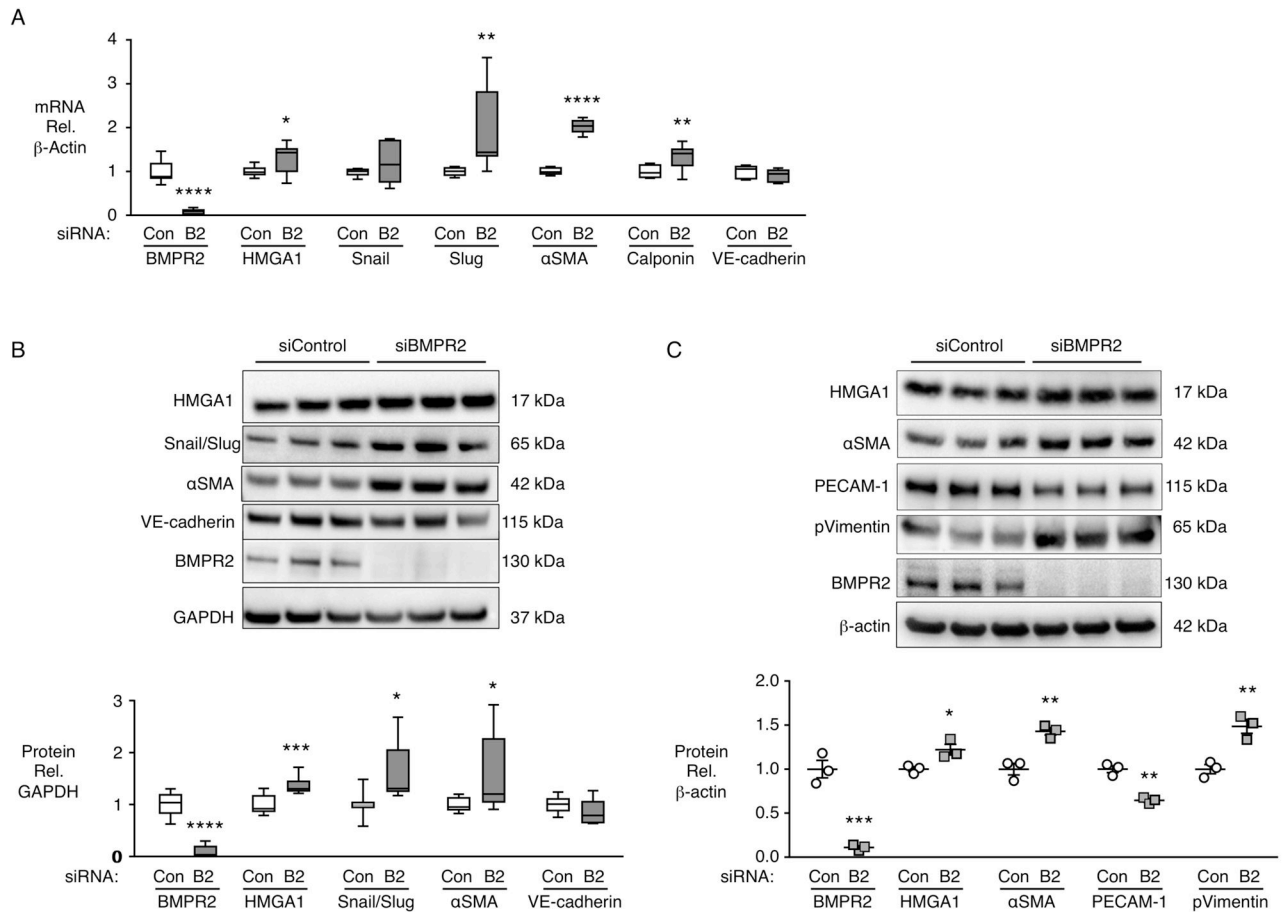


Figure 2. HMGA1 localizes to PAECs in PAH, but not in controls. Representative confocal images of different size pulmonary arteries in tissue sections from donor controls and patients with PAH stained for vWF (red), SM22 α (green), HMGA1 (white) and DRAQ7 (blue). HMGA1 co-localizes with endothelial cells (arrows) and neointimal cells (arrow heads) in tissues from patients with PAH, while the expression of HMGA1 is limited to rare cells in the PA adventitia from control donors (arrow heads). Scale bar=25 μ m (left column) and 50 μ m (middle and right columns).

**Figure 3.**

BMPR2 silencing in control PAECs induces increased HMG1 and EndMT markers. Commercially available PAECs were transfected with siRNA for BMPR2 (B2) or control non-targeting siRNA (Con). (A) Gene expression changes were assessed by qPCR after 72h. (B) Representative immunoblot and densitometric quantification of protein expression assessed 7 days after siRNA transfection. Snail/Slug indicates an antibody recognizing both Snail and Slug proteins. (C) Representative immunoblot and densitometric quantification of protein expression assessed 7 days after siRNA transfection. Boxplots indicate minimum, maximum and median for $n=9$ (A and B). Scatterplots indicate mean \pm SEM for $n=3$ (C). * $P<0.05$, ** $P<0.01$, *** $P<0.001$, **** $P<0.0001$ compared to respective Con by Student's t -test.

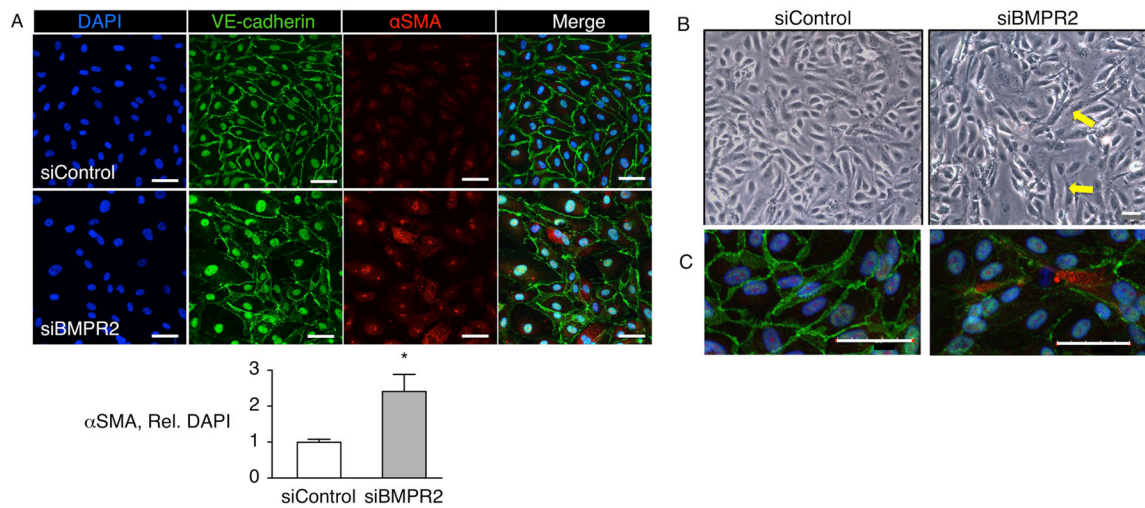
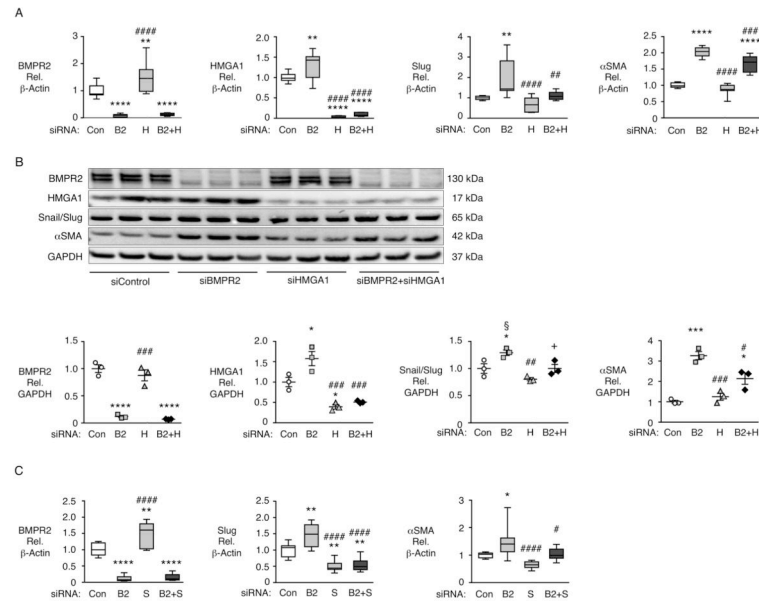


Figure 4.

Silencing of BMPR2 enhances the expression of α SMA in PAECs. Commercially available PAECs were transfected with siRNAs targeting BMPR2 or non-targeting control siRNA and analyzed after 7 days. (A) Cells were analyzed by immunofluorescence for the expression of VE-cadherin (green), α SMA (red) and nuclei (DAPI, blue). Scale Bar=50 μ m. Graph indicates quantification of α SMA immunofluorescence relative to DAPI. Bars indicate mean \pm SEM, n=5. *P<0.05. (B) Representative phase contrast light microscopy images showing typical cobblestone morphology of control siRNA transfected PAECs vs. a monolayer including cells with an elongated spindle shape (arrows) in BMPR2 siRNA transfected PAECs. Scale Bar=100 μ m. (C) Immunofluorescence microscopy showing an elongated PAEC expressing α SMA (red) from BMPR2 siRNA transfected PAECs compared to control siRNA transfected PAECs. Scale Bar=50 μ m.

**Figure 5.**

HMGA1 and Slug are necessary for EndMT gene expression changes induced by loss of BMPR2. Commercially available PAECs were transfected using non-targeting siRNA (Con) or siRNA targeting BMPR2 (B2), HMGA1 (H), BMPR2 and HMGA1 (B2+H), Slug (S), or Slug and BMPR2 (B2+S). mRNA normalized to β -actin was assessed by qPCR 72h after transfection. (A) Gene expression levels of BMPR2, HMGA1, Slug and α SMA following siRNA for BMPR2 \pm HMGA1. (B) Representative immunoblot and densitometric analysis of BMPR2, HMGA1, Snail/Slug and α SMA protein expression normalized to GAPDH 72h following siRNA for BMPR2 \pm HMGA1. (C) Gene expression levels of BMPR2, Slug and α SMA following siRNA for BMPR2 \pm Slug. Boxplots indicate minimum, maximum and median for n=9 (A and C). Scatterplots indicate mean \pm SEM for n=3 (in B). *P<0.05, **P<0.01, ***P<0.001, ****P<0.0001 by one-way ANOVA relative to Con. #P<0.05, ##P<0.01, ###P<0.001, ####P<0.0001 by one-way ANOVA relative to siRNA (B2) treatment. In Panel B, P<0.05, by one-way ANOVA with selected post-hoc comparisons of B2 vs. Con siRNA (§) and B2+H vs. B2 siRNA (+).

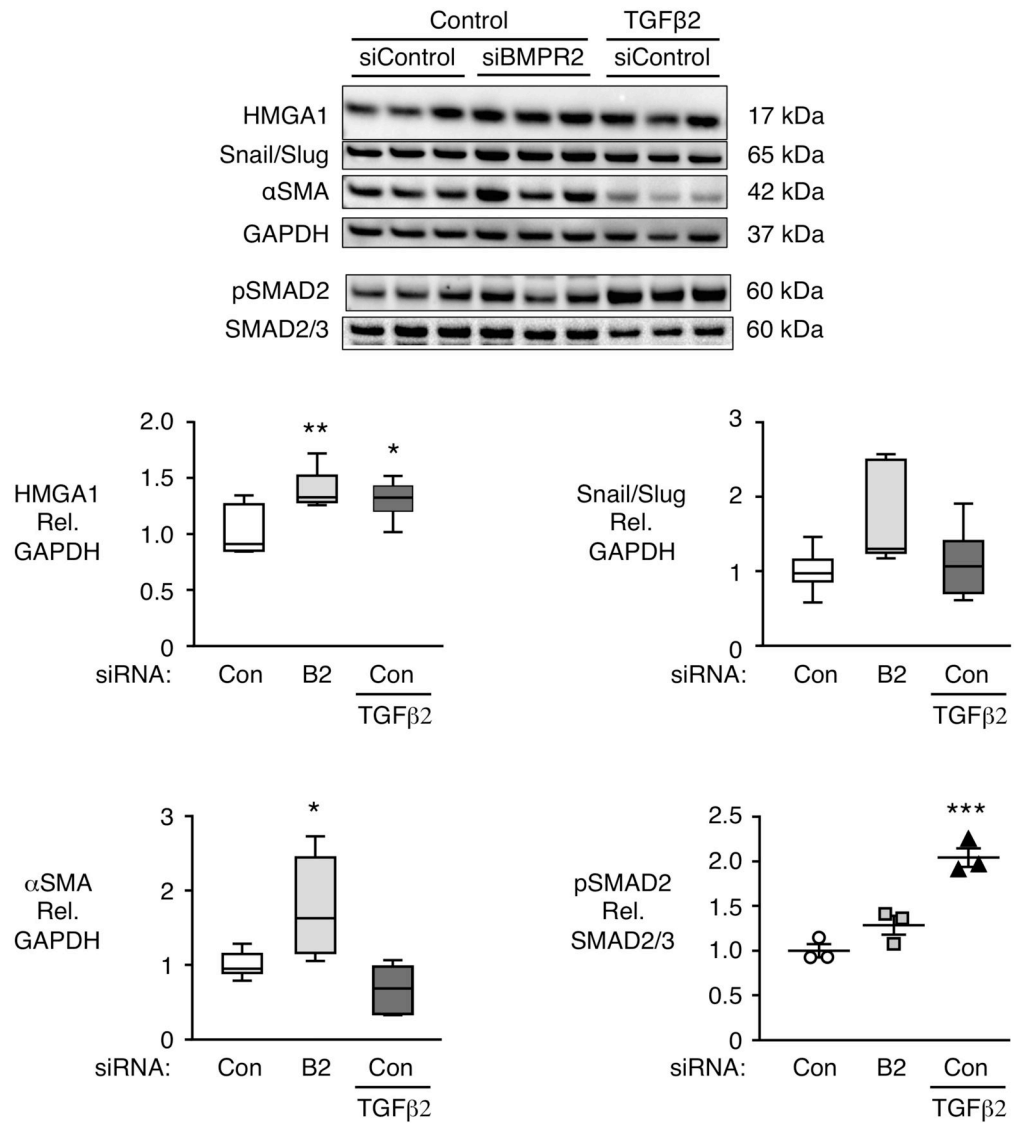
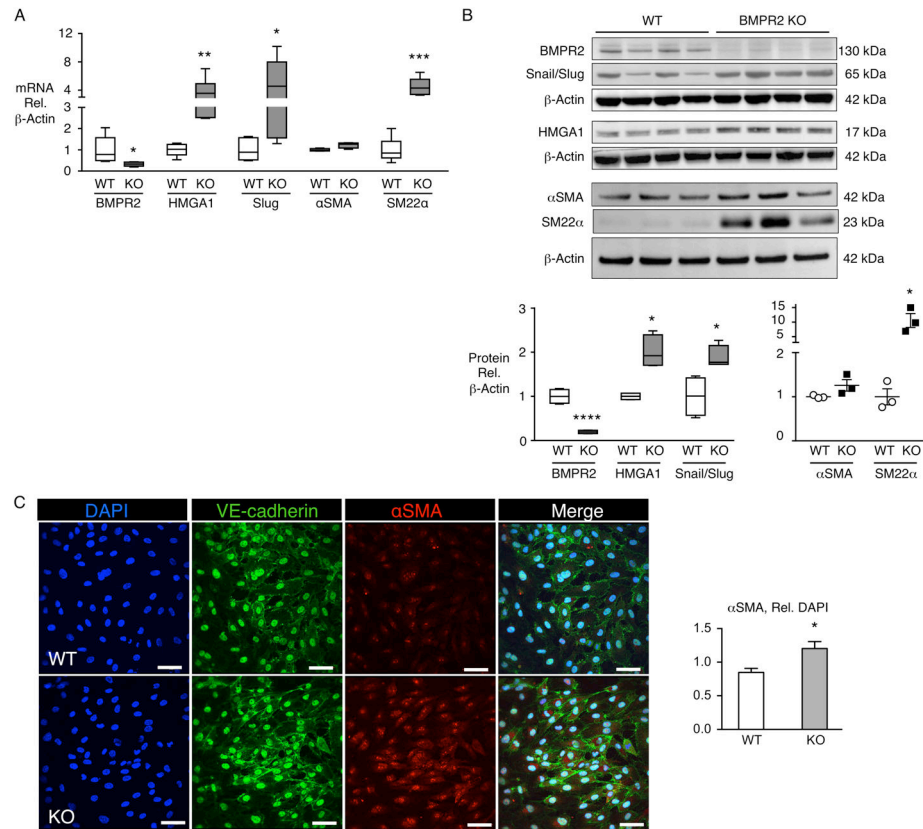


Figure 6. TGFβ2 does not induce EndMT in PAECs. Representative immunoblot with densitometric analysis of HMGA1, Snail/Slug, αSMA and pSMAD2 in control PAECs transfected with control (Con) or BMPR2 (B2) siRNA and treated with vehicle or TGFβ2 (10 ng/ml) for 5 days, starting 48h after transfection. Boxplots indicate minimum, maximum and median for n=6 per group. Scatterplot indicates mean±SEM for n=3. *P<0.05, **P<0.01, ***P<0.001 vs. non-targeting non TGFβ2-treated siRNA control by one-way ANOVA.

**Figure 7.**

Pulmonary ECs from mice lacking endothelial BMPR2 show changes consistent with EndMT. Pulmonary ECs isolated from mice with BMPR2 deleted in ECs (BMPR2 KO or KO) or wild type (WT) controls were assessed for EndMT changes at the mRNA (A) and protein (B) levels, and by immunofluorescence microscopy (C). Pulmonary ECs were isolated from three mice, pooled and cultured. Assays were conducted at passages 3–8. (A) mRNA assessed by qPCR, n=6. (B) Representative immunoblot and densitometric quantification of WT or BMPR2 KO pulmonary ECs, n=3 or 4 as shown in the two blots (passages 2–5). (C) Representative immunofluorescence images by confocal microscopy of WT or BMPR2 KO mouse pulmonary ECs for VE-cadherin (green) and α SMA (red). Nuclei stained with DAPI (blue). Scale bar=50_μm. Quantification of α SMA fluorescence is depicted below, n=3. Boxplots indicate minimum, maximum and median. Scatterplot indicates mean \pm SEM. *P<0.05, **P<0.01, ***P<0.001, ****P<0.0001 vs. control or WT by Student's t-test.

EndMT Mechanism Related to Pulmonary Arterial Hypertension

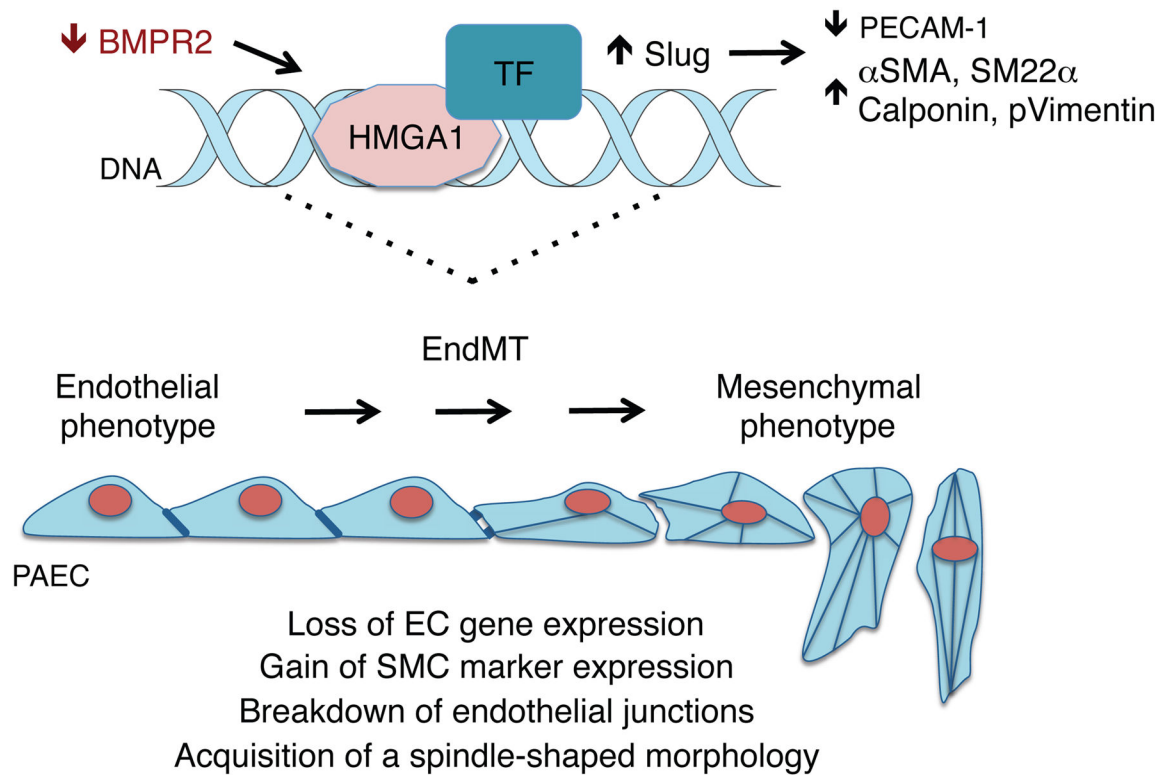


Figure 8.

Proposed model: Loss of BMPR2 promotes EndMT via HMGA1. Loss of BMPR2 in PAECs leads to heightened expression of HMGA1, which increases the transcription factor Slug. HMGA1 binds to DNA and may promote binding of additional pro-EndMT transcription factors. Expression of smooth muscle genes, such as α SMA, SM22 α , calponin and p-vimentin are increased and the endothelial gene PECAM1 is decreased, reflecting a mesenchymal phenotype.

Table 1

Characteristics of Patients and Controls.

PAH Patients											
ID	Assay	Age (Yr)	Gender	Race	Ethnicity	Diagnosis	BMPR2 Mutation	PAP s/d/m	PVR (WU)	6MW (m)	PAH Medications
PAH-01	IHC WB	33	F	White	Non-Hispanic	FPAH	Yes	87/29/48	9.74	288	bosentan, treprostini, sildenafil, epo, prosteno
PAH-02	IHC WB	40	F	White	Non-Hispanic	IPAH	No	84/26/47	N/A	294	ambrisentan, sildenafil, ilo, prost, epo, prosteno
PAH-03	IHC WB	27	M	White	Non-Hispanic	IPAH	No	90/51/68	11.38	423.7	bosentan, sildenafil, epo, prosteno
PAH-04	IHC WB	49	F	White	Non-Hispanic	IPAH	No	100/50/75	16.76	326.1	Ambrisentan, sildenafil, epo, prosteno
PAH-05	IHC WB	56	F	White	Non-Hispanic	FPAH	No	110/55/75	N/A	372.2	epo, prosteno, bosentan, ambrisentan, sildenafil
PAH-06	IHC	62	F	White	Non-Hispanic	IPAH	No	73/34/47	6.17	259.4	epo, prosteno, ambrisentan, bosentan
PAH-07	IHC	33	F	Black/AA	Non-Hispanic	FPAH	Yes	75/33/48	15.57	326.1	epo, prosteno, bosentan, sildenafil, treprostini
PAH-08	IHC	58	F	White	Non-Hispanic	APAH	No	127/59/77	N/A	1016	bosentan, treprostini
PAH-09	WB	16	F	White	Non-Hispanic	IPAH	N/A	104/67/80	N/A	348.4	bosentan, ambrisentan, epo, prosteno, sildenafil, treprostini
PAH-10	WB	29	F	Black/AA	Non-Hispanic	IPAH	No	63/29/41	N/A	339.2	epo, prosteno, ambrisentan, sildenafil
PAH-11	WB	37	M	White	Non-Hispanic	FPAH	Yes	119/51/77	14.22	309	sildenafil, sitaxsentan, ambrisentan, epo, prosteno, Imatinib (investi. medication), treprostini
PAH-12	WB	56	F	White	Non-Hispanic	IPAH	No	83/39/57	11.41	137.2	sildenafil, ambrisentan, treprostini
PAH-13	WB	54	F	White	Non-Hispanic	IPAH	N/A	100/45/60	N/A	296.3	sildenafil, epo, prosteno, ambrisentan, bosentan
PAH-14	WB	55	F	Black/AA	Non-Hispanic	IPAH	No	89/41/53	12.29	273.4	sildenafil, bosentan, epo, prosteno
PAH-15	WB	32	F	White	Non-Hispanic	IPAH	No	68/38/49	15.34	238	bosentan, epo, prosteno
PAH-16	WB	41	F	White	Non-Hispanic	IPAH	N/A	75/43/55	9.84	472.4	sildenafil, bosentan, epo, prosteno
PAH-17	WB	56	M	White	Non-Hispanic	IPAH	No	125/50/75	9.58	234.7	tadalafil, bosentan
PAH-18	WB	27	F	White	Non-Hispanic	IPAH	Yes	110/49/69	12.11	359.7	sildenafil, treprostini, bosentan, ilo, prost
PAH-19	WB	15	F	White	Non-Hispanic	IPAH	No	175/66/102	25.24	387	sildenafil, epo, prosteno
PAH-20	WB	25	M	White	Hispanic	IPAH	No	65/15/36	N/A	510.5	epo, prosteno, sildenafil, treprostini

Controls (Unused Donor Lungs)						
ID	Assay	Age (Yr)	Gender	Race	Ethnicity	Cause of Death
CON-01	IHC WB	11	M	White	Non-Hispanic	Anoxia-Declared Brain Dead-Natural Causes (Hanging)
CON-02	IHC WB	19	M	Black or African American	Not Reported	Anoxia of brain
CON-03	IHC	49	M	White	Unknown	Intracranial hemorrhage
CON-04	IHC	41	F	White	Non-Hispanic	Grade 4 subarachnoid hemorrhage, ruptured anterior cerebral artery aneurysm
CON-05	IHC	26	M	White	Non-Hispanic	Cerebrovascular/Stroke
CON-06	IHC	14	M	White	Non-Hispanic	Cardiac Arrest secondary to Diabetic Ketoacidosis
CON-07	WB	55	M	White	Non-Hispanic	Anoxia/cardiovascular/natural causes
CON-08	WB	24	M	White	Non-Hispanic	Cerebrovascular Stroke/Intracranial hemorrhage
CON-09	WB	40	F	White	Non-Hispanic	Extensive intracranial injury/subarachnoid hemorrhage secondary to MVA
CON-10	WB	25	M	White	Non-Hispanic	Intracranial Hemorrhage
CON-11	WB	52	F	White	Unknown	Hypoxic brain death secondary to PEA arrest
CON-12	WB	1	M	White	Non-Hispanic	Anoxia/Drowning
CON-13	WB	57	F	White	Non-Hispanic	Acute Myocardial Infarction
CON-14	WB	45	F	White	Non-Hispanic	Subarachnoid hemorrhage
CON-15	WB	56	F	White	Non-Hispanic	CVA
CON-16	WB	43	M	White	Non-Hispanic	Fatal gun shot to head

Hemodynamic data from catheterization were obtained from studies performed closest to transplantation. PAH medications are listed according to total drug exposure during treatment period of follow-up, not necessarily in combination.

IHC, Immunohistochemistry

WB, Western blots

N/A – data not available

IPAH, Idiopathic PAH

HPAH, hereditary PAH

PAP, pulmonary artery pressure (mmHg); s: systolic, d: diastolic, m: mean

PVR, pulmonary vascular resistance ($\text{dynes}/\text{sec}\cdot\text{cm}^{-5}$) (Baseline Fick PVR)

6MW, distance (m) walked in 6 minutes